2003

Probing O VI Emission in the Halos of Edge-on Spiral Galaxies

B Otte

EM Murphy

JC Howk

QD Wang
University of Massachusetts - Amherst

WR Oegerle

See next page for additional authors

Recommended Citation
Otte, B; Murphy, EM; Howk, JC; Wang, QD; Oegerle, WR; and Sembach, KR, "Probing O VI Emission in the Halos of Edge-on Spiral Galaxies" (2003). *The Astrophysical Journal*. 1010.
10.1086/375535

accepted for publication in Astrophysical Journal

Probing O VI Emission in the Halos of Edge-on Spiral Galaxies

B. Otte[1], E. M. Murphy[2], J. C. Howk[3], Q. D. Wang[4], W. R. Oegerle[5], K. R. Sembach[6]

ABSTRACT

We have used the *Far Ultraviolet Spectroscopic Explorer* to search for O VI $\lambda\lambda$1031.926, 1037.617 emission in the halos of the edge-on spiral galaxies NGC 4631 and NGC 891. In NGC 4631, we detected O VI in emission toward a soft X-ray bubble above a region containing numerous Hα arcs and filaments. The line-of-sight component of the motion of the O VI gas appears to match the underlying disk rotation. The observed O VI luminosities can account for 0.2−2% of the total energy input from supernovae (assuming a full O VI emitting halo) and yield mass flux cooling rates between 0.48 and 2.8 $M_\odot\,yr^{-1}$ depending on the model used in the derivations. Based on these findings, we believe it is likely that we are seeing cooling, galactic fountain gas. No emission was detected from the halo of NGC 891, a galaxy in a direction with considerably high foreground Galactic extinction.

Subject headings: ISM: general — ISM: individual (NGC 4631, NGC 891) — galaxies: general — galaxies: halos — galaxies: individual (NGC 4631, NGC 891) — galaxies: ISM

[1]Department of Physics and Astronomy, The Johns Hopkins University, 3400 N. Charles St., Baltimore, MD 21218; otte@pha.jhu.edu

[2]Department of Astronomy, University of Virginia, Charlottesville, VA 22903; emurphy@virginia.edu

[3]CASS, University of California-San Diego, 9500 Gilman Dr., La Jolla, CA 92093; howk@ucsd.edu

[4]Department of Astronomy, University of Massachusetts, Amherst, MA 01003; wqd@astro.umass.edu

[5]Laboratory for Astronomy and Solar Physics, NASA/GSFC, Greenbelt, MD 20771; oegerle@uvo.gsfc.nasa.gov

[6]Space Telescope Science Institute, 3700 San Martin Dr., Baltimore, MD 21218; sembach@stsci.edu

1. INTRODUCTION

In a seminal work, Spitzer (1956) predicted that the Milky Way is surrounded by a tenuous, hot corona. Provided that the temperature of such gas was below the escape temperature for a galaxy, he showed that the gas should extend several kiloparsecs above the midplane. Spitzer's original arguments have been extended to a more general theory of the dynamical evolution of the gaseous disks of spiral galaxies. This so called "galactic fountain" model (Shapiro & Field 1976; Bregman 1980) postulates that the hot gas produced by multiple overlapping supernovae would be buoyant in the thin, cold disks of gas in spiral galaxies. As the hot gas rises from the thin disk into the halo, it cools, perhaps forming condensations of neutral material which then fall back towards the thin disk as high- or intermediate-velocity clouds.

The existence of such gas in the Milky Way is now well documented through observations of strong O VI absorption (e.g. Savage et al. 2000) and X-ray emission (Burrows & Mendenhall 1991). The 1032/1038 Å doublet transition of Li-like oxygen (O VI) is an important tracer of hot, collisionally ionized material. At temperatures of $\sim 3 \times 10^5$ K, where gas of near-solar metallicity cools most efficiently, emission from the O VI doublet can be the primary coolant. Hence, observations of O VI emission provide a direct probe of the cooling rate of material near this temperature. Furthermore, because the cooling of gas at temperatures of a few times 10^5 K is so much more efficient than that of material at higher (or lower) temperatures, O VI emission traces rapidly cooling material that may condense into clouds in the galactic fountain scenario. Observations of O VI from this "transition temperature" gas in the halos of galaxies provide fundamental information on the circulation of material within spiral galaxies.

An O VI absorption line survey of the Milky Way (Savage et al. 2003) showed that the observed O VI was best explained by a patchy disk corotating with the Galactic plane with signs of outflows. O VI observed in emission in the Milky Way has been associated with gas in or around the Local Bubble (Welsh et al. 2002 and references therein) and an outflow from the Perseus arm (Otte, Dixon, & Sankrit 2003). With our improving understanding of the O VI distribution inside the Milky Way, it becomes necessary to search for O VI emission in other galaxies as well in order to be able to distinguish between peculiarities and common properties of galaxies. We analyzed spectra of two galaxies (NGC 4631 and NGC 891) taken by the *Far Ultraviolet Spectroscopic Explorer (FUSE)*. Both galaxies are nearly edge-on (i.e. allow clear distinction between disk and halo gas) and known for strong extraplanar emission in radio continuum, optical lines, and soft X-rays (SXR). Thus, they appear to be good candidates to search for evidence of galactic fountains. While the spectra of NGC 891 did not reveal any O VI emission, we detected the O VI doublet in NGC 4631.

This is the first detection of O VI in emission in a spiral galaxy other than the Milky Way and its companions.

2. OBSERVATIONS AND DATA REDUCTION

2.1. NGC 4631

We obtained spectra with the low resolution aperture ($30'' \times 30''$) of *FUSE* at two positions above the disk of NGC 4631 (see Figure 1) as part of Project P134. Position A is at the peak of the 1/4 keV X-ray emission detected by Wang et al. (1995) using *ROSAT*. Position B is between two Hα arcs that were believed to form the walls of an open chimney into the halo (Rand, Kulkarni, & Hester 1992), although a recent *Hubble Space Telescope* Hα image (Wang et al. 2001) indicates that this feature may be a superposition of several loops. All *FUSE* observations were conducted in TTAG mode where the detectors record the arrival time, x- and y-position, and the pulse height of each event (Sahnow et al. 2000). About 2/3 of each observation was conducted during orbital night.

The O VI lines in the NGC 4631 spectra were extracted from the raw data files. Only events with a pulse height between 4 and 15, inclusive, were used in the analysis. Nearby O I airglow lines were used to determine the height of the extraction windows, and the spectra were summed perpendicular to the dispersion direction. Emission free regions adjacent to the O VI lines in the dispersion direction were used to determine the background.

Figure 2 shows a plot of the extracted spectra for both pointings toward NGC 4631. The wavelength scale was determined by running the spectra through the *FUSE* data pipeline V2.0.5. Its uncertainty is about one pixel (0.007 Å). Both the redshifted 1032 Å and 1038 Å line were detected on the LiF1A channel. However, the latter was blended with the O I $\lambda\lambda$ 1039.23,1040.94,1041.69 airglow triplet. The background at wavelengths > 1040 Å was increased due to a stripe of scattered light within the satellite. The O VI emission lines were also seen on the LiF2B segment for Position B; however, the lower effective area significantly reduced the quality of the data. Therefore, we have used only data from the 1032 Å emission line of segment LiF1A in the analysis.

A comparison of day-plus-night versus night-only data yielded the same flux in the O VI λ1032 line and therefore ruled out the possibility that the emission arose from scattered solar O VI emission in the LiF channels. Deep integrations towards other lines of sight ruled out detector artifacts, scattered light, and stray light contamination at the positions of the detected lines. The background was not significantly higher during the sunlit portion of the orbit; therefore, we have used the combined day and night data in our analysis. The

resulting signal-to-noise ratios for the integrated O VI λ1032 intensities are 4.5 (Position A) and 6.0 (Position B).

2.2. NGC 891

The data for NGC 891 were obtained as part of *FUSE* Guest Investigator Cycle 2 program B114. Two positions below the disk and one position above the bulge of NGC 891 (see Figure 3) were observed. The data reduction was identical to the data reduction for NGC 4631 above. Approximately 85% of the observations were conducted during the night portion of the orbit. The observational data for both galaxies are listed in Table 1. Given the large random errors in the intensities of NGC 891, we do not believe that any of these detections are significant.

3. RESULTS

3.1. NGC 4631

NGC 4631 is an Sc/SBd type galaxy at a distance of about 7.6 Mpc with an inclination of $i \approx 85°$. The interaction between NGC 4631 and its two neighboring galaxies NGC 4656 and NGC 4627 might have triggered the active star formation observed in NGC 4631 today. The galaxy possesses a complex system of Hα filaments and bubbles (Wang et al. 2001) and an extended radio halo with spurs up to 10 kpc above the disk (Hummel & Dettmar 1990). X-ray observations of NGC 4631 revealed a SXR bubble on the north side of the disk (Wang et al. 1995) and a halo of gas extending up to 8 kpc above the plane with temperatures of $(2-7) \times 10^6$ K (Wang et al. 2001). Both the radio and the X-ray halo appear asymmetric with the larger extent being on the north side of the disk.

The two *FUSE* pointings for NGC 4631 were chosen to lie within the SXR bubble observed with *ROSAT* (Wang et al. 1995, see Figure 1). Assuming an effective area of 27.0 cm^2 for the LiF1A segment and 900 arcs^2 for the aperture area, we derive O VI λ1032 intensities of 4600 ± 1000 photons s^{-1} cm^{-2} sr^{-1} (Position A) and 8000 ± 1300 photons s^{-1} cm^{-2} sr^{-1} (Position B). Table 2 lists the intensities (also converted to ergs s^{-1} cm^{-2} sr^{-1}) and the corresponding height above the disk. The O VI λ1032 intensity at Position B is a factor of five smaller than the 2 σ upper limit of Ferguson et al. (1995), who observed the southern portion of the galaxy with the *Hopkins Ultraviolet Telescope* on the Astro-2 mission. The full extent of the O VI emitting gas is unknown. However, it is useful to consider two cases. In the first scenario, the O VI emission is confined to the region of the SXR bubble on the north side of

the disk. On the other hand, the O VI emission may extend across the full hot halo revealed by the *Chandra* observations of Wang et al. (2001). The former would correspond to a single large bubble breaking out into the halo, while the latter implies a full galactic fountain. Therefore, we will calculate the luminosity for both cases assuming that the average O VI surface brightness is equivalent to the average of Positions A and B. The O VI λ1032/O VI λ1038 line ratio approaches two in optically thin gas and is reduced in optically thick gas due to self-absorption. We assumed the upper limit for this line ratio of 2 in order to account for the O VI λ1038 emission in our calculations. Ignoring extinction (see below) we calculated a lower limit for the total O VI luminosity of $L_{\rm OVI} = (6.2 \pm 0.8) \times 10^{38}\,{\rm ergs\,s^{-1}}$ for the bubble and $L_{\rm OVI} = (2.3 \pm 0.3) \times 10^{39}\,{\rm ergs\,s^{-1}}$ for the entire halo.

3.1.1. Correction for Extinction

The Milky Way extinction toward NGC 4631 is $E(B-V) = 0.017$ (Schlegel, Finkbeiner, & Davis 1998). Using a Galactic extinction curve by Cardelli, Clayton, & Mathis (1989), we derived an optical depth $\tau = 0.25$, i.e. the UV flux is attenuated by a factor of 1.28. The corrected values for the luminosities are $L_{\rm OVI} = (7.9 \pm 1.1) \times 10^{38}\,{\rm ergs\,s^{-1}}$ for the bubble and $L_{\rm OVI} = (3.0 \pm 0.4) \times 10^{39}\,{\rm ergs\,s^{-1}}$ for the entire halo. The amount of extinction within NGC 4631 is uncertain. Long slit optical spectroscopy of the Balmer lines by Martin & Kern (2001) has revealed evidence for significant and patchy extinction due to dust in the halo of NGC 4631 up to 5 kpc from the plane. However, another group found almost no extinction at a height of > 1 kpc on the northern side of the disk (Otte et al. 2001). We obtained long slit spectra of NGC 4631 with the 2.3 m Steward Observatory on Kitt Peak, Arizona, on 2002 April 7–9. The slit was about $4\farcs5$ wide and orientated north-south to cross both *FUSE* positions. The measured Hα/Hβ line ratios are comparable to those measured by Otte et al. (2001). We therefore assume that extinction within the halo of NGC 4631 is negligible.

3.1.2. Comparison with X-ray Luminosity

As mentioned earlier, the O VI emission is an important coolant for hot ionized gas. In fact, for gas in heating-cooling equilibrium, the O VI emission cooling at intermediate temperatures (few $\times 10^5$ K) should dominate the radiative cooling in the SXR emission of 10^6 K gas (Sutherland & Dopita 1993). The SXR intensities in the $0.1 - 2$ keV range measured by *Chandra* and integrated over the area of the *FUSE* positions are $1.5 \times 10^{-7}\,{\rm ergs\,s^{-1}\,cm^{-2}\,sr^{-1}}$ (Position A) and $3.1 \times 10^{-7}\,{\rm ergs\,s^{-1}\,cm^{-2}\,sr^{-1}}$ (Position B) yielding SXR/O VI ratios of 1.2 ± 0.3 and 1.3 ± 0.2 for Positions A and B, i.e. the intensities are more or less comparable

between the O VI doublet and the SXR emission. However, the used O VI $\lambda\lambda$1032,1038 emission was a lower limit (see paragraph 3.1) and not corrected for Galactic extinction (because we did not know the Galactic extinction for the SXR emission); the SXR/O VI ratios did not account for any dust in NGC 4631 either. Thus, the quoted ratios are probably lower limits suggesting that the gas is not in equilibrium.

The total O VI luminosity (corrected for Galactic extinction, see paragraph 3.1.1), if assumed to cover the whole halo of NGC 4631, is by a factor of 9 lower than the two component fit of the X-ray luminosity ($2.7 \times 10^{40}\,\mathrm{ergs\,s^{-1}}$, Wang et al. 1995, corrected for different distances). The corresponding temperature of this X-ray luminosity was approximately 6×10^5 K, i.e. a temperature about twice as high as the one for the peak of the O VI cooling curve. This again implies that the gas is not cooling efficiently in O VI, i.e. it is not in equilibrium. However, the uncertainties here are higher than for the comparison above, as we now have compared observational data with a model using different simplifications (e.g. for the shape and extent of the emitting halo).

Wang et al. (1995) estimated that the mechanical energy input from supernovae is about $(1.5 - 15) \times 10^{41}\,\mathrm{ergs\,s^{-1}}$, i.e. the observed O VI luminosity can account for at most $\sim 2\,\%$ of the total energy input from supernovae. If the gas is in equilibrium, then the remaining energy input has to be used to transport the gas from the disk into the halo against the gravitational potential of the galaxy and against the pressure of the magnetic field lines and is partially lost due to cooling of $\sim 10^6$ K hot gas by species other than oxygen. From the cooling flow models of Edgar & Chevalier (1986), we calculate that the full halo case is equivalent to a mass flux of $2.8\,\mathrm{M_\odot\,yr^{-1}}$ for cooling at constant density and $1.8\,\mathrm{M_\odot\,yr^{-1}}$ for cooling at constant pressure. In case of a single cooling bubble the corresponding mass fluxes are $0.74\,\mathrm{M_\odot\,yr^{-1}}$ (isochoric) and $0.48\,\mathrm{M_\odot\,yr^{-1}}$ (isobaric). A rough estimate for the mass flux derived from *ROSAT* observations is $\sim 1\,\mathrm{M_\odot\,yr^{-1}}$ (Wang et al. 1995). Despite the large uncertainties due to unknown extinction and the differences in the cooling models, the data suggest that the O VI emitting region is larger than the SXR bubble, but smaller (within a factor of ~ 2) than the X-ray halo observed with *Chandra*. This means that outflows are more significant in the central region of the galaxy, as indicated by the filamentary structure in the Hα image (Wang et al. 2001). If, in fact, there was strong, patchy extinction along our lines of sight, the actual O VI luminosities could be much higher than the observed luminosities and could account for a significant fraction of the input energy from supernovae. On the other hand, if the O VI emission originated in the interface between cold clouds moving through the hot coronal gas, the relationship between SXR and O VI emission would become more complicated.

3.1.3. Rotation Velocity

We fitted the observed O VI λ1032 emission line by a convolution of a tophat (106 km s^{-1} wide to represent the filled *FUSE* 30″ × 30″ square aperture) and a Gaussian profile (to represent the spectral resolution of *FUSE*). We used χ^2 calculations to determine the best central wavelengths and intrinsic velocity dispersions for the emission lines at Positions A and B. In order to estimate 1 σ uncertainties for these parameters, we varied each parameter independently until the corresponding minimum χ^2 increased by 1 relative to the best fit χ^2. The derived values are $\lambda_c = 1034.30 \pm 0.09$ Å and FWHM $= 200 \pm 50$ km s^{-1} for Position A and $\lambda_c = 1034.37 \pm 0.08$ Å and FWHM $= 170 \pm 50$ km s^{-1} for Position B. The corresponding radial velocities (geocentric) are $v = 690 \pm 30$ km s^{-1} (Position A) and 710 ± 20 km s^{-1} (Position B). An offset of -9.1 and -9.5 km s^{-1}, respectively, yields local standard of rest velocities. If the O VI emitting gas does not fill the LWRS aperture and is not centered in it, the maximum additional offset in the line centroid is 50 km s^{-1} (for a point source at the border of the aperture). The line broadening due to the satellite's orbital motion is < 8 km s^{-1}, i.e. well within the uncertainties of the FWHM.

The intrinsic FWHMs, if assumed to be thermal widths, correspond to temperatures of $(1.4 \pm 0.7) \times 10^7$ K (Position A) and $(1.0 \pm 0.6) \times 10^7$ K (Position B). These temperatures are an order of magnitude higher than the hottest component of the SXR emission. This suggests that the line widths are caused by turbulent motion or differential rotation rather than thermal motion. From position-velocity diagrams (Rand 1994), one can expect an offset of about 50–100 km s^{-1} between the systemic velocity (606 km s^{-1}) and the velocity of gas corotating in the disk at the distances of the *FUSE* positions projected onto the major axis. A combination of the size of the low resolution aperture (30″ or about 1.1 kpc) and differential rotation yields a velocity dispersion of up to 200 km s^{-1} in the galactic plane near the center. The O VI velocity centroids and FWHMs closely match those of the H I gas in the disk of NGC 4631. Thus, the line-of-sight component of the motion of the O VI emitting gas appears to follow the rotation of the underlying disk gas. Due to the galaxy's high inclination, the velocity of the O VI emitting gas perpendicular to the disk is unknown. Although not conclusive, this strong relationship to the disk gas implies that the O VI emitting material originated in the disk.

3.1.4. Scale Height

If the gas has an exponential distribution in the vertical direction above the disk, we can calculate the density scale height of the gas from the two observations at Positions A

and B using:

$$h = \frac{-2(z_{\rm A} - z_{\rm B})}{\ln(\frac{I_{\rm A}}{I_{\rm B}})} \tag{1}$$

where $z_{\rm A}$ and $z_{\rm B}$ are the vertical heights of the projected aperture above the plane of the galaxy, and $I_{\rm A}$ and $I_{\rm B}$ are the measured specific intensities at Positions A and B, respectively. The 2 in Equation 1 results from the fact that the intensity is proportional to the square of the density. Using the intensities and z heights from Table 2, we find

$$h = 8.3 \pm 4.1\,{\rm kpc}. \tag{2}$$

The large uncertainty in the density scale height results from the large uncertainties in the measured specific intensities at Positions A and B. However, it appears that the scale height of O VI gas in NGC 4631 is significantly larger than the 2.3 kpc scale height found by Savage et al. (2003) for the Milky Way. Using the intensities from paragraph 3.1.2, we find a scale height of about 6.6 kpc for the SXR emission in NGC 4631, whereas Hummel, Beck, & Dahlem (1991) reported a scale height of about 8 kpc for the magnetic field. Scale heights derived from optical emission lines range between 0.9 and 1.2 kpc, not considering the roughly constant intensity at $z > 3$ kpc (Martin & Kern 2001). Given the uncertainties, the scale heights of the O VI and SXR emission and the magnetic field appear to be comparable.

3.2. NGC 891

The Sb spiral galaxy NGC 891 is at a distance of about 9.6 Mpc with an inclination of $i \geq 88.6°$ (Rupen et al. 1987). We observed three positions in the halo of NGC 891 and did not detect O VI in emission to a level greater than 3σ (Fig. 4). The 3σ intensity limits can be obtained from Table 2. The Milky Way extinction in this direction is $E(B-V) = 0.065$ (Schlegel et al. 1998). Assuming a standard interstellar extinction curve (Cardelli et al. 1989), the UV flux is attenuated by a factor of 2.4 ($\tau = 0.88$). If we assume that the O VI emitting halo of NGC 891 is the same size as the X-ray emitting halo seen by Bregman & Pildis (1994), and that the average specific intensity of the halo in NGC 891 is equal to the average at Positions 1 and 2, then the upper limit to the O VI λ1032 luminosity is $L_{1032} < 7.5 \times 10^{38}\,{\rm ergs\,s^{-1}}$. Bregman & Houck (1997) found that the SXR (0.1–2.5 keV) band luminosity is $2.45 \times 10^{39}\,{\rm ergs\,s^{-1}}$ with a cooling rate of 0.08 $M_\odot\,{\rm yr^{-1}}$ (corrected for $d = 9.6$ Mpc). This predicts an O VI λ1032 luminosity (Edgar & Chevalier 1986) of $5.7 \times 10^{37}\,{\rm ergs\,s^{-1}}$ (isochoric) and $8.8 \times 10^{37}\,{\rm ergs\,s^{-1}}$ (isobaric), well within our limits. We have not attempted any correction for extinction in the halo of NGC 891 itself.

4. CONCLUSIONS

NGC 4631 has a stronger radio halo than NGC 891, but a comparable far-IR luminosity. Rand, Kulkarni, & Hester (1992) concluded from these observations that NGC 4631 probably has a larger star formation rate than NGC 891. The *Hubble Space Telescope* images of Wang et al. (2001) clearly show loops, arcs, and filaments as would be expected from galactic chimneys. *ROSAT* observations (Wang et al. 1995) revealed the presence of a large region of SXR emission directly above the arcs and filaments, indicating that some of the hot supernovae gas has vented into the halo. In this paper, we reported the detection of O VI emission at two locations above the arcs at the peaks of the SXR emission with a line-of-sight velocity similar to the disk gas and a FWHM broader than what might be expected from thermal motions of hot gas. The observation of O VI emitting gas suggests that the hot gas originated in the disk and is cooling. Due to the large uncertainties in the O VI intensities and luminosities and the range in the luminosities and mass flux rates predicted by cooling flow models, it is not clear whether the cooling flow in NGC 4631 is (yet) in equilibrium with the mass flux derived from X-ray observations. However, given all this evidence, we believe that, because of its edge-on nature, NGC 4631 is the first spiral galaxy in which O VI has been detected in emission unambiguously from the galactic halo and in which all the expected components for a full cycle of gas in a galactic fountain have been observed. The lack of reliable O VI measurements for NGC 891 is likely explained with the large foreground extinction of the Milky Way and the amount of dust in NGC 891 itself. The O VI luminosities predicted from cooling flow models are well within our 3σ limits for NGC 891.

The NGC 4631 data were obtained for the Guaranteed Time Team by the NASA-CNES-CSA *FUSE* mission operated by the Johns Hopkins University. Financial support to U. S. participants has been provided by NASA contract NAS5-32985. The NGC 891 data were obtained as part of the *FUSE* Cycle 2 Guest Investigator Program B114. Financial support to U. S. participants has been provided by NASA contract NAG5-10250. JCH recognizes support from NASA grant NAG5-10957. This work made use of the NASA Extragalactic Database (NED) and the NASA Astrophysics Data System (ADS).

REFERENCES

Bregman, J. N. 1980, ApJ, 236, 577

Bregman, J. N., & Houck, J. C. 1997, ApJ, 485, 159

Bregman, J. N., & Pildis, R. A. 1994, ApJ, 420, 570

Burrows, D. N., & Mendenhall, J. A. 1991, Nature, 351, 629

Cardelli, J. A., Clayton, G. C., & Mathis, J. S. 1989, ApJ, 345, 245

Edgar, R. J., & Chevalier, R. A. 1986, ApJ, 310, L27

Ferguson, H. C., Dixon, W. V., Davidsen, A. F., & Dettmar, R.–J. 1995, ApJ, 454, L23

Howk, J. C., & Savage, B. D. 2000, AJ, 119, 644

Hummel, E., Beck, R., & Dahlem, M. 1991, A&A, 248, 23

Hummel, E., & Dettmar, R.-J. 1990, A&A, 236, 33

Martin, C., & Kern, B. 2001, ApJ, 555, 258

Otte, B., Dixon, W. V., & Sankrit, R. 2003, ApJL, 586, in press

Otte, B., Reynolds, R. J., Gallagher, J. S., & Ferguson, A. M. N. 2001, ApJ, 560, 207

Rand, R. J. 1994, A&A, 285, 833

Rand, R. J., Kulkarni, S. R., & Hester, J. J. 1992, ApJ, 396, 97

Rupen, M. P., van Gorkom, J. H., Knapp, G. R., Gunn, J. E., & Schneider, D. P. 1987, AJ, 94, 61

Sahnow, D. J., et al. 2000, ApJ, 538, L7

Sancisi, R., & Allen, R. J. 1979, A&A, 74, 73

Savage, B. D., et al. 2000, ApJ, 538, L27

Savage, B. D., et al. 2003, ApJS, in press

Schlegel, D. J., Finkbeiner, D. P., & Davis, M. 1998, ApJ, 500, 525

Shapiro, P. R., & Field, G. B. 1976, ApJ, 205, 762

Spitzer, L. 1956, ApJ, 124, 20

Sutherland, R. S., & Dopita, M. A. 1993, ApJS, 88, 253

Wang, Q. D., Immler, S., Walterbos, R., Lauroesch, J. T., & Breitschwerdt, D. 2001, ApJ, 555, L99

Wang, Q. D., Walterbos, R. A. M., Steakley, M. F., Norman, C. A., & Braun, R. 1995, ApJ, 439, 176

Welsh, B. Y., Sallmen, S., Sfeir, D., Shelton, R. L., & Lallement, R. 2002, A&A, 394, 691

Table 1. OBSERVATIONS

Position	Program ID	Right Ascension (J2000 h m s)	Declination (J2000 ° ′ ″)	Exposure Time (s)	Events in LiF1A 1032 Å line
NGC4631–A	P1340101	12 42 08.8	32 34 36.0	20954	55 ± 12
NGC4631–B	P1340201	12 42 08.8	32 33 36.0	16220	74 ± 12
NGC891–1	B1140101	02 22 29.0	42 21 12.0	31603	15 ± 12
NGC891–2	B1140201	02 22 40.0	42 22 36.0	31513	25 ± 13
NGC891–3	B1140301	02 22 44.8	42 22 12.0	18531	12 ± 10

Table 2. SPECIFIC O VI λ1032 INTENSITIES

Position	z	I_{1032}	
	(kpc)	(photons s^{-1} cm^{-2} sr^{-1})	(10^{-8} ergs s^{-1} cm^{-2} sr^{-1})
NGC4631–A	4.8	4600 ± 1000	9 ± 2
NGC4631–B	2.5	8000 ± 1300	15 ± 3
NGC891–1[a]	2.4	< 2000	< 3.8
NGC891–2[a]	1.4	< 2200	< 4.2
NGC891–3[a]	4.1	< 2800	< 5.5

[a]The listed intensity is a 3σ upper limit.

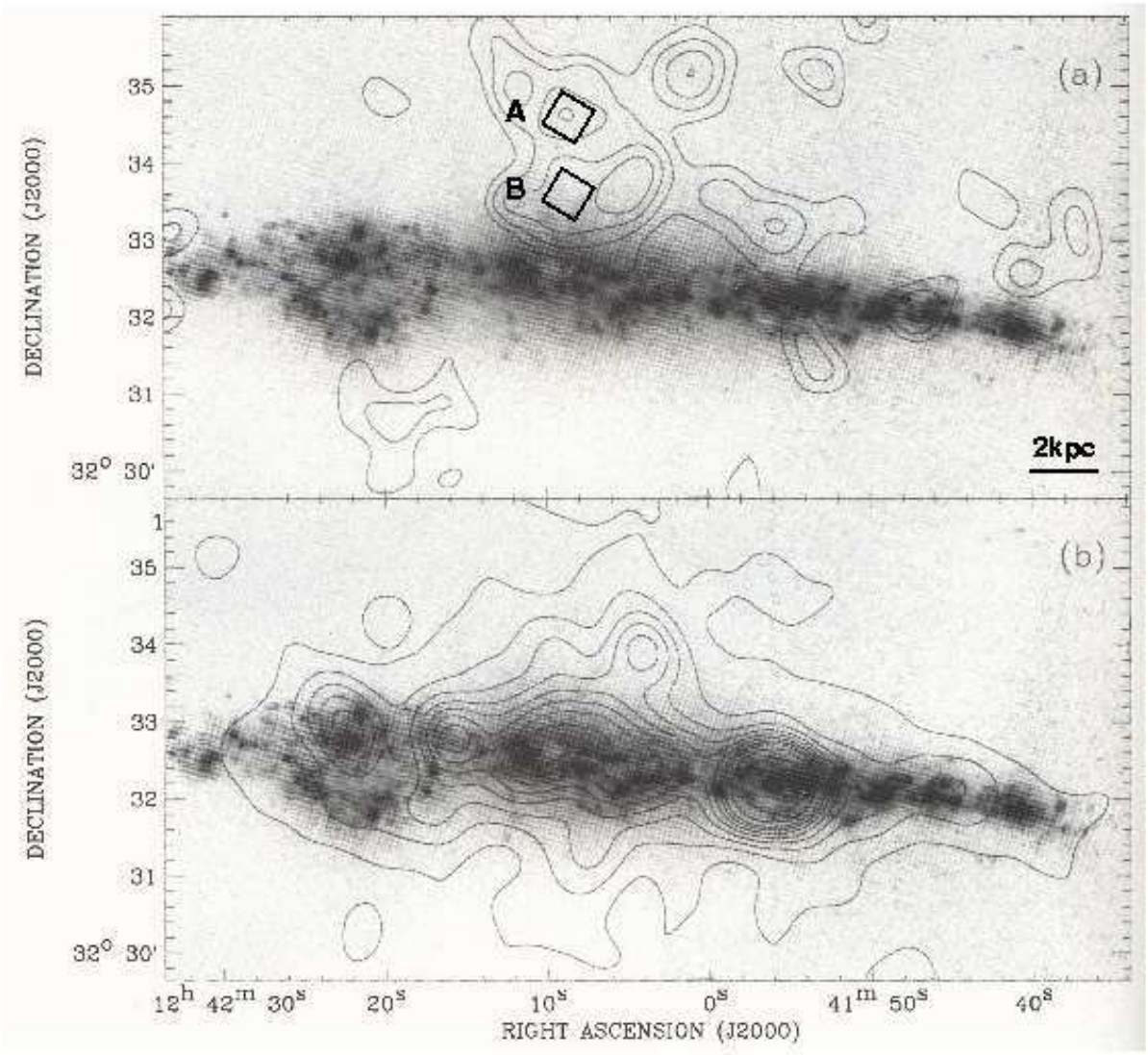

Fig. 1.— X-ray contours superimposed on an Hα image of NGC 4631 (Wang et al. 1995). Both *FUSE* positions are marked in the top panel, which shows the SXR bubble observed in the *ROSAT* 0.15–0.3 keV band. The bottom panel shows the hard X-ray contours of the 0.5–2.0 keV band overlaid over the same Hα image as in the top panel.

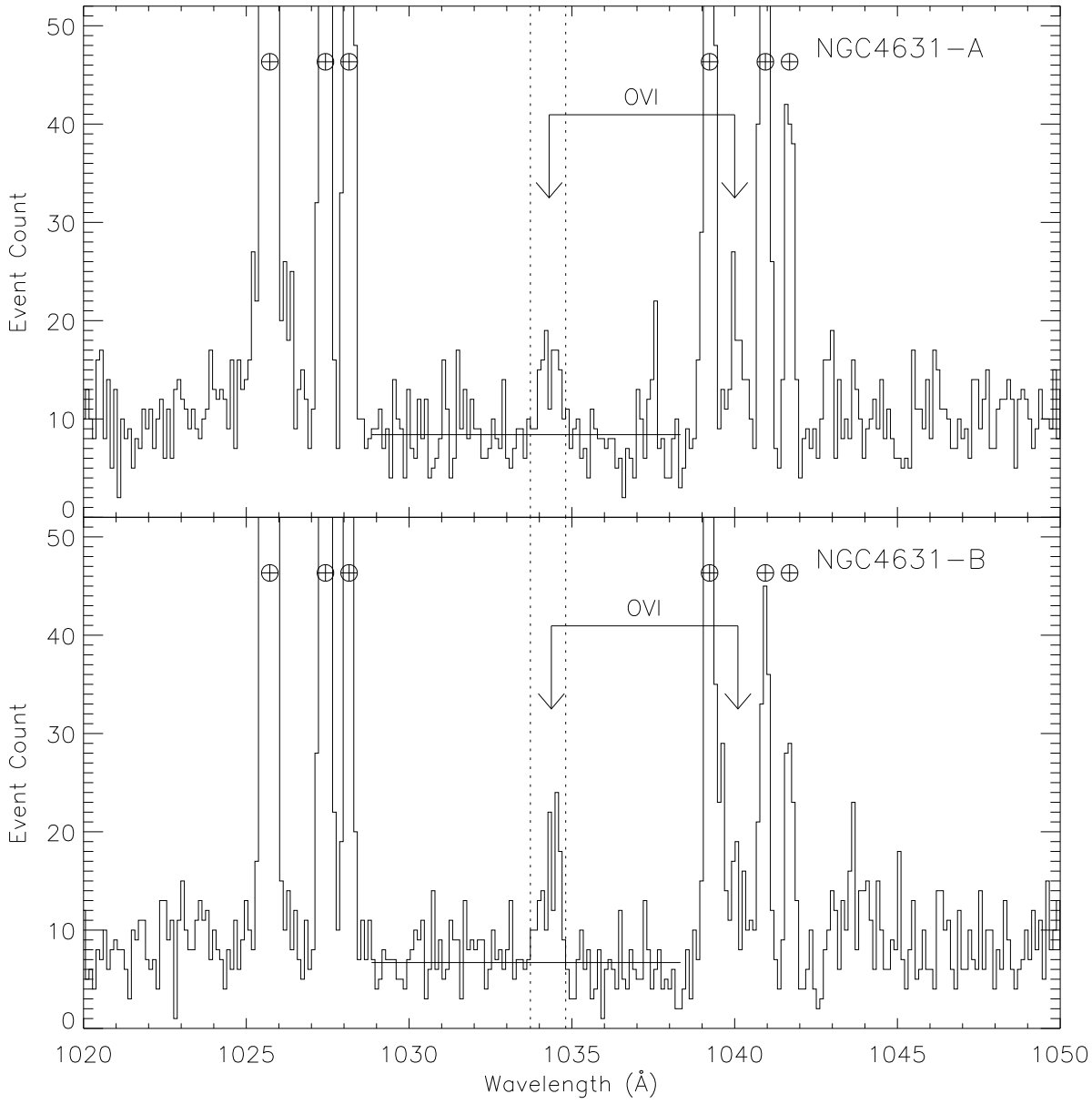

Fig. 2.— *FUSE* day-plus-night spectra of NGC 4631 at Positions A (top) and B (bottom). The spectra were binned by 16 pixels for display only. The O VI $\lambda\lambda$1032,1038 doublet is marked with arrows; airglow lines are marked with the Earth symbol. The dashed lines show the extraction window over which the O VI λ1032 photons were counted. The continuum fit for this emission line is plotted as a horizontal line. Its extend outside the dashed lines shows the region of the spectrum used to determine the continuum.

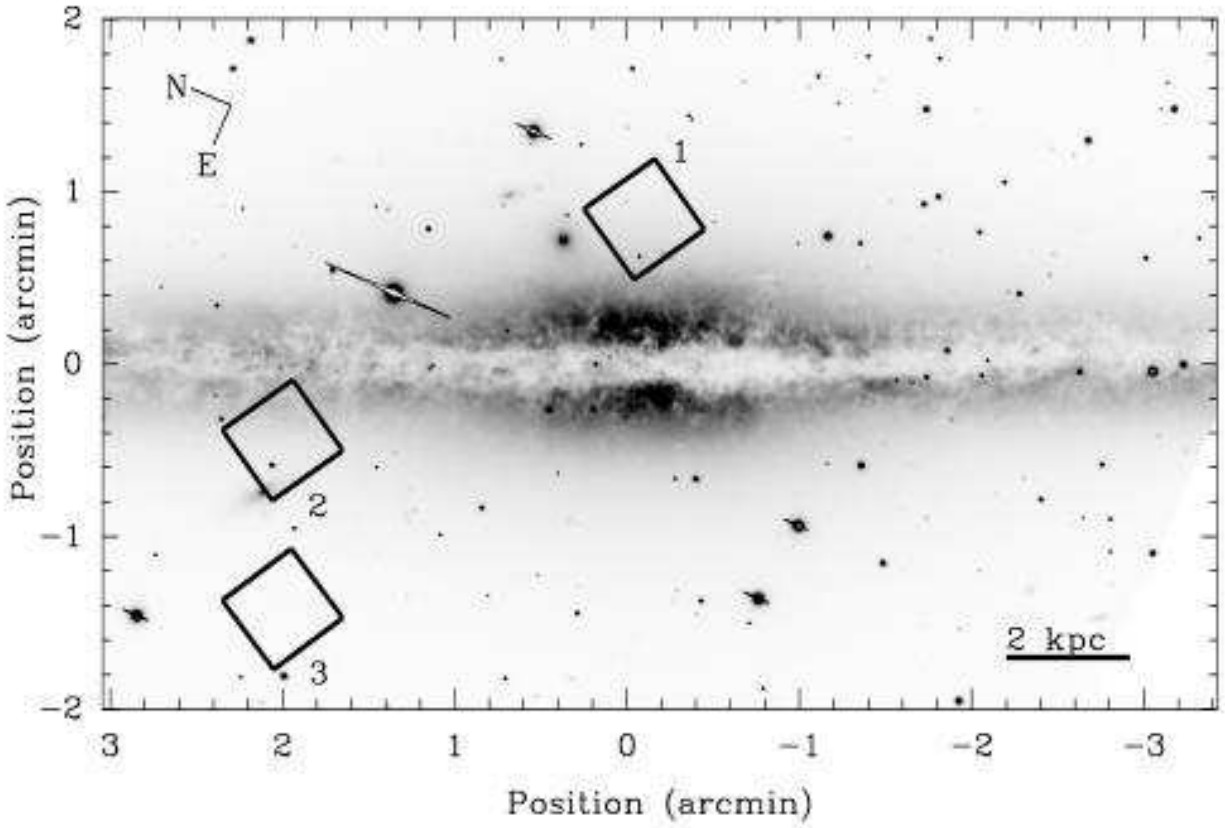

Fig. 3.— *BV* image of NGC 891 (Howk & Savage 2000). The three *FUSE* positions are marked.

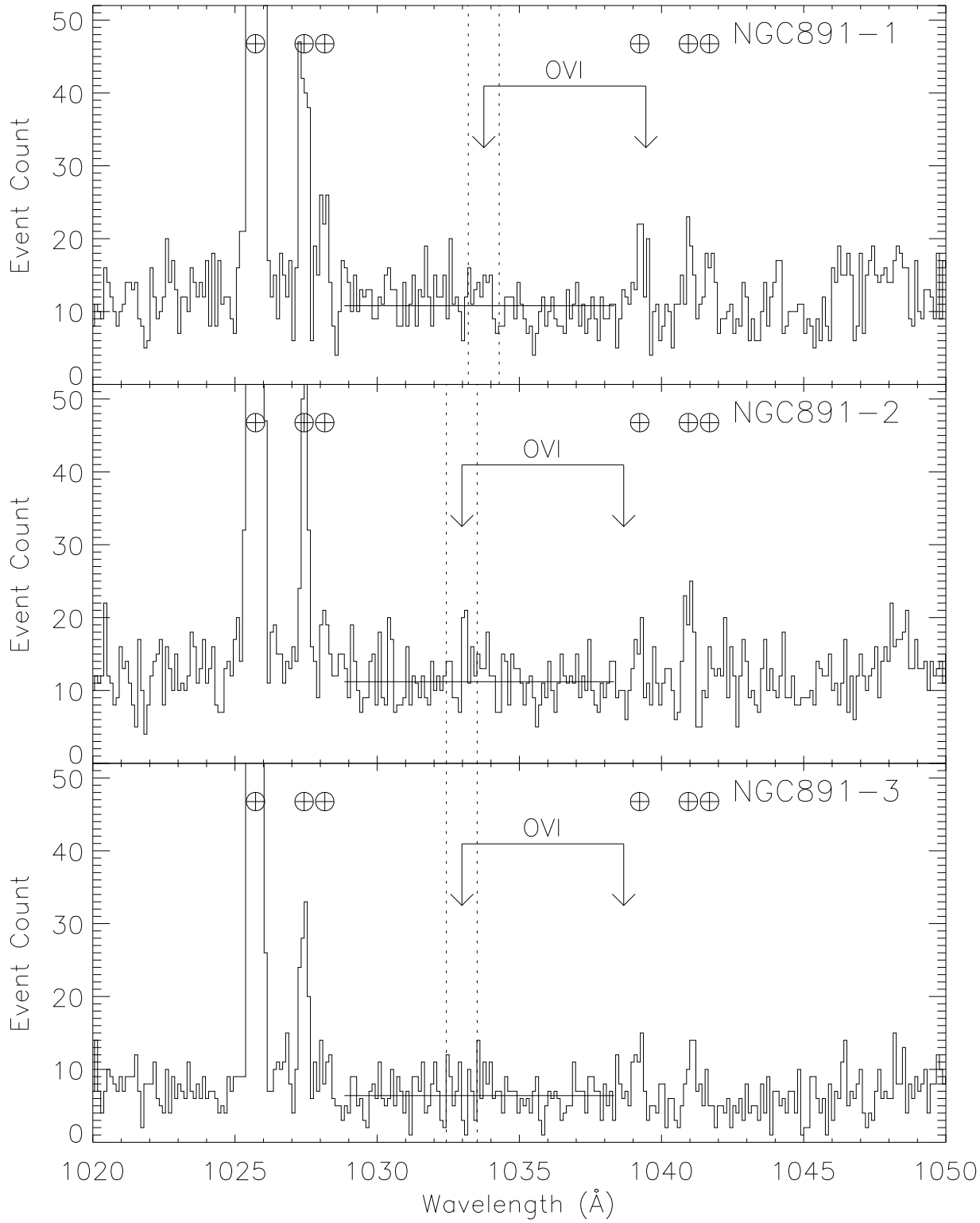

Fig. 4.— Same as Fig. 2, but for NGC 891 at Positions 1–3 (from top to bottom). The positions of the arrows and extraction windows are based on the rotation curve by Sancisi & Allen (1979).